Additive Model for ^{119}Sn Mössbauer Quadrupole Splitting in Five-co-ordinate Organotin(IV) Compounds

By **G. Michael Bancroft, V. G. Kumar Das,** and **Tsun K. Sham,** Department of Chemistry, University of Western Ontario, London N6A 3K7, Canada
Michael G. Clark,* Royal Radar Establishment, Malvern, Worcestershire WR14 3PS

Mössbauer parameters are reported for ten cationic organotin(IV) complexes of type $[R_3SnL_2][BPh_4]$ (R = alkyl or phenyl, L = electronegative ligand). Details are given of a regression method which is used to distinguish structural isomers of trigonal-bipyramidal $[R_3SnL_2]$ species by their ^{119}Sn quadrupole splittings. By use of new and literature data, partial quadrupole splitting (p.q.s.) parameters are calculated for a variety of ligands in trigonal-bipyramidal structures. Comparison of theory with experiment indicates that the additive model gives a consistent account of the relationship between quadrupole splitting and stereochemistry in trigonal-bipyramidal organotin(IV) compounds. The ^{119}Sn parameters are used to calculate p.q.s. parameters for $^{121}Sb^{V}$, thus extending recent work on application of the additive model to five-co-ordinate organoantimony(V) compounds.

THE additive model for interpretation of electric field gradients (e.f.g.) [1,2] provides a powerful method for obtaining structural information from ^{119}Sn Mössbauer quadrupole splittings of organotin(IV) compounds.[3] However, its application to trigonal-bipyramidal co-ordination has been hindered by the necessity to assign different parameters to apical and equatorial ligands.[1] Recently, we reported preliminary details of a novel regression procedure which overcomes this difficulty.[4] In the present paper theoretical details of this regression method are given, and partial quadrupole splitting (p.q.s.) values are derived for many commonly occurring ligands and applied to problems in the structural chemistry of five-co-ordinate tin(IV).

Since the quadrupole coupling constant ratio for the ^{119}Sn and ^{121}Sb Mössbauer resonances in isoelectronic isostructural compounds is well established,[5,6] we are able to deduce p.q.s. parameters for organoantimony(V) compounds. These values are used to extend the recent work of Ruddick *et al.*[7]

For reasons which have already been detailed elsewhere,[1,2] we make no attempt to calculate effects due to distortions from ideal trigonal-bipyramidal geometry. However, since a systematic association between distortion and stoicheiometry has been established in at least one case [8] we attempt to weight data for different stoicheiometries about equally in the calculation of p.q.s. parameters. By this strategy any biassing effect of such distortions is minimized.

EXPERIMENTAL AND RESULTS

Five- and six-co-ordinate organotin(IV) compounds were prepared and characterized as reported elsewhere.[6,9-11] ^{119}Sn Mössbauer spectra were obtained at 80 K by use of a 5 mCi $BaSnO_3$ source at room temperature, and an Austin Science Associates spectrometer; calibration and computation procedures have been described previously.[6,12] Magnetic spectra at 4.2 K and 6 T for $[Ph_3Sn(bzbz)]$ (bzbz = anion of dibenzoylmethane) and $[Me_3Sn(bipyo)][BPh_4]$ (bipyo = 2,2′-bipyridine *NN*′-dioxide) (Figure 1) were taken and computed at the P.C.M.U., Harwell.

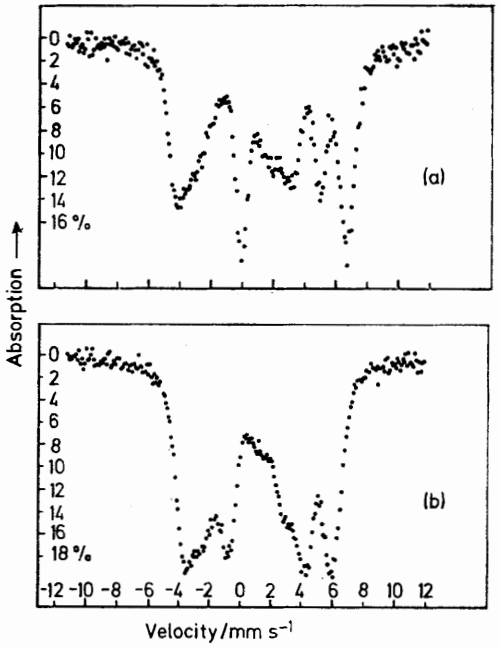

FIGURE 1 Mössbauer–Zeeman spectra of (a) $[Me_3Sn(bipyo)][BPh_4]$ and (b) $[Ph_3Sn(bzbz)]$. Spectra were taken at 4.2 K in a transverse applied magnetic field of 6 tesla

Quadrupole splittings and centre shifts for new cationic five-co-ordinate compounds are given in Table 1. The centre shifts are typical of the $[R_3Sn^{IV}]$ moiety, but show

[1] M. G. Clark, A. G. Maddock, and R. H. Platt, *J.C.S. Dalton*, 1972, 281.
[2] M. G. Clark, in 'Molecular Structure and Properties,' ed. A. D. Buckingham, *M.T.P. Internat. Rev. Sci., Phys. Chem. Ser.* **2**, vol. 2, ch. 7, Butterworths, London, 1975.
[3] G. M. Bancroft and R. H. Platt, *Adv. Inorg. Chem. Radiochem.*, 1972, **15**, 59.
[4] G. M. Bancroft, V. G. Kumar Das, T. K. Sham, and M. G. Clark, *J.C.S. Chem. Comm.*, 1974, 236.
[5] G. M. Bancroft, K. D. Butler, and E. T. Libbey, *J.C.S. Dalton*, 1972, 2643.
[6] G. M. Bancroft, V. G. Kumar Das, and K. D. Butler, *J.C.S. Dalton*, 1974, 2355.
[7] J. N. R. Ruddick, J. R. Sams, and J. C. Scott, *Inorg. Chem.*, 1974, **13**, 1503.
[8] R. J. Dickinson, R. V. Parish, P. J. Rowbotham, A. R. Manning, and P. Hackett, *J.C.S. Dalton*, 1975, 424.
[9] V. G. Kumar Das and W. Kitching, *J. Organometallic Chem.*, 1967, **10**, 57.
[10] V. G. Kumar Das, W. Kitching, and C. J. Moore, *J. Organometallic Chem.*, 1970, **22**, 399.
[11] V. G. Kumar Das, *Inorg. Nuclear Chem. Letters*, 1970, **9**, 155, and to be published.
[12] G. M. Bancroft, B. W. Davis, N. C. Payne, and T. K. Sham, *J.C.S. Dalton*, in the press.

no particular trend and will not be discussed further. The quadrupole coupling data, together with other results taken from the literature, give the regressions [4] displayed in Figure 2 and discussed below. The structural assignments given in Figures 2 and 3 are supported by *X*-ray studies for isomer (II) [$Ph_3Sn(bzbz)$] [12] and isomer (I) (Me_3SnL_2; L = unidentate).[13] There are no *X*-ray data yet to support our assignment of isomer (III), but the ν(Sn–C) i.r. data [11] are consistent with this assignment, and the Mössbauer quadrupole splittings (*vide infra*) strongly support our assignment of isomer (III) in Figure 2. Table 2 summarizes all new and literature data used in the regression analysis and the calculation of p.q.s. parameters for $^{119}Sn^{IV}$.

The Mössbauer–Zeeman experiments on [$Me_3Sn(bipyo)$]-[BPh_4] [structure (III) in Figure 3] and [$Ph_3Sn(bzbz)$] [structure (II)] show that the sign of e^2qQ is negative in both cases, with η values of 0.23 ± 0.1 and 0.48 ± 0.1,

TABLE 1

Mössbauer parameters for five-co-ordinate cationic tin(IV) compounds *

Compound †	Centre shift ‡/ mm s^{-1}	Quad. split.§/ mm s^{-1}	Linewidths/ mm s^{-1} Γ_1	Γ_2
[$Me_3Sn(Ph_3PO)_2$][BPh_4]	1.28	3.87	0.97	1.01
[$Me_3Sn(hmpa)_2$][BPh_4]	1.34	3.85	1.03	1.11
[$Me_3Sn(dmso)_2$][BPh_4]	1.30	3.63	1.13	1.07
[$Ph_3Sn(dmso)_2$][BPh_4]	1.27	3.39	1.05	1.07
[$Me_3Sn(Ph_3AsO)_2$][BPh_4]	1.18	3.29	1.15	0.97
[$Me_3Sn(opo)$][BPh_4]	1.37	4.10	1.04	1.05
[$Ph_3Sn(opo)$][BPh_4]	1.22	3.52	1.03	1.05
[$Me_3Sn(diphoso)$][BPh_4]	1.31	3.90	1.00	1.15
[$Me_3Sn(baso)$][BPh_4]	1.24	3.69	1.11	1.01
[$Me_3Sn(bipyo)$][BPh_4]	1.32	−3.67 (η = 0.23 ± 0.1)	1.14	1.11

* All measurements at 80 K; χ^2 is 500 ± 5 0with *ca.* 500 degrees of freedom; estimated error ±0.03 mm s^{-1}. For the ^{119}Sn 23.88 keV Mössbauer resonance 1 mm s^{-1} = 19.26 MHz. † hmpa = Hexamethylphosphoramide; dmso = dimethyl sulphoxide; opo = methylenebis(diphenylphosphine oxide); diphoso = ethylenebis(diphenylphosphine oxide); baso = methylenebis(diphenylarsine oxide); bipyo = 2,2′-bipyridine *N′N*-dioxide. ‡ Relative to $BaSnO_3$. § Where sign and η are not recorded they have not been determined experimentally.

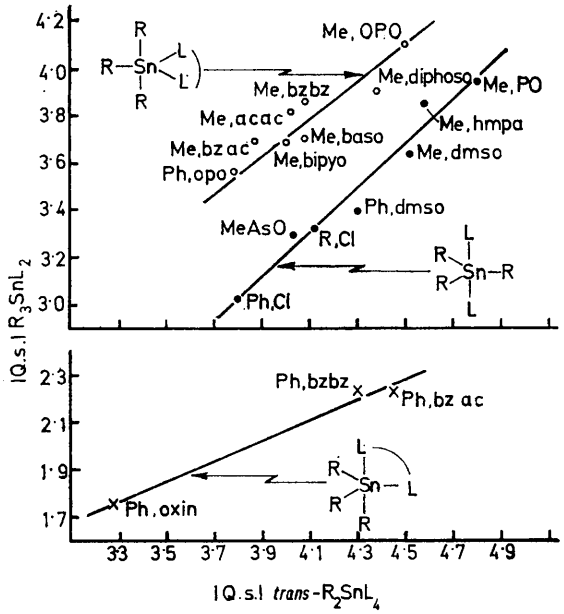

FIGURE 2 Magnitude of ^{119}Sn quadruple splitting in [R_3SnL_2] plotted against magnitude of splitting in *trans*-[R_2SnL_4] (or twice *cis*-[R_3SnL_4]). Units are mm s^{-1}; for ligand abbreviations see footnotes to Tables 1 and 2. The lines are least-squares fits discussed in the text

TABLE 2

^{119}Sn Mössbauer quadrupole splitting data used in regression analysis and calculation of p.q.s. parameters

Code no.*	Compound ●	Obs. q.s. †
(i) *trans*-oct.*		
(1)	[$Me_2Sn(Ph_3PO)_4$][BPh_4]$_2$ [a]	(+)4.75
(2)	[$Me_2Sn(hmpa)_4$][BPh_4]$_2$ [a]	(+)4.58
(3)	[$Me_2Sn(dmso)_4$][BPh_4]$_2$ [a]	(+)4.52
(4)	[(alkyl)$_2SnCl_4$]$^{2-}$ [b]	+ 4.12
(5)	[$Me_2Sn(Ph_3AsO)_4$][BPh_4]$_2$ [a]	(+)4.03
(6)	[$Ph_2Sn(dmso)_4$][BPh_4]$_2$ [a]	(+)4.30
(7)	(pyH)$_2$[Ph_2SnCl_4] [c]	(+)3.80
(8)	[$Me_2Sn(opo)_2$][BPh_4]$_2$ [a]	(+)4.50
(9)	[$Me_2Sn(diphoso)_2$][BPh_4]$_2$ [a]	(+)4.38
(10)	[$Me_2Sn(baso)_2$][BPh_4]$_2$ [a]	(+)4.08
(11)	[$Me_2Sn(bipyo)_2$][BPh_4]$_2$ [a]	(+)4.00
(12)	[$Me_2Sn(acac)_2$] [b,d]	+ 4.02
(13)	[$Me_2Sn(bzbz)_2$] [d]	+ 4.08
(14)	[$Me_2Sn(bzac)_2$] [d]	+ 3.87
(15)	[$Ph_2Sn(opo)_2$][BPh_4]$_2$ [a]	(+)3.78
(ii) *cis*-oct.		
(16)	[$Ph_2Sn(oxin)_2$] [o,p]	+ 1.64
(17)	[$Ph_2Sn(bzbz)_2$] [d]	(−)2.15
(18)	[$Ph_2Sn(bzac)_2$] [d]	(−)2.23
(19)	[(alkyl)$_2Sn(oxin)_2$] [o,p]	+ 2.00
(iii) (I)		
(101)	[$Me_3Sn(Ph_3PO)_2$][BPh_4] [u]	(−)3.87
(102)	[$Me_3Sn(hmpa)_2$][BPh_4] [u]	(−)3.85
(103)	[$Me_3Sn(dmso)_2$][BPh_4] [u]	(−)3.63
(104)	[(alkyl)$_3SnCl_2$]$^-$ [b]	− 3.31
(105)	[$Me_3Sn(Ph_3AsO)_2$][BPh_4] [u]	(−)3.29
(106)	[$Ph_3Sn(dmso)_2$][BPh_4] [u]	(−)3.39
(107)	[Ph_3SnCl_2]$^-$ [b]	− 3.02
(108)	[$Ph_3Sn(hmpa)_2$][BPh_4] [g]	(−)3.51
(109)	[$Me_3Sn(dmf)_2$][BPh_4] [g]	(−)3.90
(110)	[$Me_3Sn(H_2O)_2$][BPh_4] [h]	(−)4.10
(111)	[$Me_3SnCl(dma)$] [i]	(−)3.69
(112)	[$Me_3SnCl(py)$] [o]	(−)3.44
(113)	[$Me_3SnBr(py)$] [j]	(−)3.18
(114)	[$Ph_3SnCl(pyO)$] [k]	(−)2.94
(115)	[$Ph_3Sn(NCS)(pyO)$] [k]	(−)3.14
(116)	[Me_3SnF] [b]	(−)3.82
(117)	[Me_3SnI] [b]	(−)3.05
(118)	[$Me_3Sn(OH)$] [b,l,r]	− 2.88
(119)	[Me_3SnCN] [b]	(−)3.12
(120)	[Me_3SnN_3] [b,l]	(−)3.52
(121)	[$Ph_3SnNO_3(dmso)$] [g]	(−)3.40
(122)	[$Ph_3SnNO_3(hmpa)$] [g]	(−)3.33
(123)	[$Me_3Sn(OAc)_3$] [m,s]	− 3.68
(124)	[$Me_3Sn(OCOCH_2I)$] [m]	(−)3.83
(125)	[$Me_3Sn(OCOCH_2Br)$] [m]	(−)3.90
(126)	[$Me_3Sn(OCOCH_2Cl)$] [m]	(−)3.89
(127)	[$Me_3Sn(OCOCBr_3)$] [m]	(−)4.13
(128)	[$Me_3Sn(OCOCCl_3)$] [m]	(−)4.15
(129)	[$Me_3Sn(OCOCHCl_2)$] [m]	(−)4.08
(130)	[$Me_3Sn(OCOCF_3)$] [m]	(−)4.22
(131)	[$Me_3Sn(OCOH)$] [b]	(−)3.55
(132)	[$Me_3Sn(SO_3CF_3)$] [n]	(−)4.57
(133)	[$Me_3Sn(SO_3Me)$] [n]	(−)4.21
(134)	[$Me_3Sn(ONOR)$] [t]	(−)3.37
(135)	[$Ph_3SnCl(pip)$] [q]	− 2.95
(iv) (II)		
(201)	[$Ph_3Sn(oxin)$] [e,s]	− 1.75
(202)	[$Ph_3Sn(bzbz)$] [f]	− 2.25
(203)	[$Ph_3Sn(bzac)$] [f]	(+)2.25

[13] B. Y. K. Ho and J. J. Zuckerman, *J. Organometallic Chem.*, 1973, **49**, 1.

TABLE 2 (*Continued*)

Code no.*	Compound *	Obs. q.s. †
(v) (III)		
(301)	$[Me_3Sn(opo)][BPh_4]$ [u]	(−)4.10
(302)	$[Me_3Sn(diphoso)][BPh_4]$ [u]	(−)3.90
(303)	$[Me_3Sn(baso)][BPh_4]$ [u]	(−)3.69
(304)	$[Me_3Sn(bipyo)][BPh_4]$ [u]	− 3.67
(305)	$[Me_3Sn(acac)]$ [f]	(−)3.81
(306)	$[Me_3Sn(bzbz)]$ [f]	(−)3.86
(307)	$[Me_3Sn(bzac)]$ [f]	(−)3.69
(308)	$[Ph_3Sn(opo)][BPh_4]$ [u]	(−)3.52

* (1)—(19) octahedral; (101)—(135), (201)—(203), and (301)—(308) trigonal-bipyramidal isomers (I), (II), and (III), respectively. See Table 1 footnotes for abbreviations; acac = anion of acetylacetone; bzbz = anion of dibenzoylmethane; bzac = anion of benzoylacetone; oxin = anion of 8-hydroxyquinoline; dmf = dimethylformamide; dma = dimethylacetamide; py = pyridine; pyO = pyridine *N*-oxide; pyH = pyridinium; pip = piperidine. † $\frac{1}{2}ce^2qQ(1 + \frac{1}{3}\eta^2)^{\frac{1}{2}}E\gamma^{-1}$ in mm s^{-1}. Values are unweighted means, where appropriate, of measurements at *ca.* 80 K. Where no measured sign is available, the additive-model predicted sign is given in parentheses (although it may be unreliable, particularly if *cis*-phenyl groups are present).

[a] Ref. 6. [b] Mean of values collected in ref. 3. [c] B. W. Fitzsimmons, N. J. Seeley, and A. W. Smith, *J. Chem. Soc.* (*A*), 1969, 143. [d] G. M. Bancroft and T. K. Sham, *Canad. J. Chem.*, 1974, **52**, 1361. [e] R. C. Poller and J. N. R. Ruddick, *J. Chem. Soc.* (*A*), 1969, 2273. [f] Ref. 12. [g] G. M. Bancroft and V. G. Kumar Das. [h] Ref. 24. [i] J. C. Hill, R. S. Drago, and R. H. Herber, *J. Amer. Chem. Soc.*, 1969, **91**, 1644. [j] J. Nasielski, N. Sprecher, J. de Vooght, and S. Lejeune, *J. Organometallic Chem.*, 1967, **8**, 97. [k] Ref. 26 and R. W. J. Wedd and J. R. Sams, *Canad. J. Chem.*, 1970, **48**, 71. [l] N. Bertazzi, G. Alonzo, R. Barbieri, and R. H. Herber, *J. Organometallic Chem.*, 1974, **65**, 23. [m] C. Poder and J. R. Sams, *J. Organometallic Chem.*, 1969, **19**, 67. [n] J. R. Sams, in *M.T.P. Internat. Rev. Sci. Phys. Chem. Ser.* 1, vol. 4 (Magnetic Resonance, ed. C. A. McDowell), Butterworths, London, p. 85. [o] Mean of values collected in P. J. Smith, *Organometallic Chem. Rev.* (*A*), 1970, **5**, 373. [p] Ref. 23. [q] B. A. Goodman, N. N. Greenwood, K. L. Jaura, and K. K. Sharma, *J. Chem. Soc.* (*A*), 1971, 1865. [r] B. A. Goodman and N. N. Greenwood, *J. Chem. Soc.* (*A*), 1971, 1862. [s] Ref. 14. [t] J. Lorbeth, J. Pebler, and G. Lange, *J. Organometallic Chem.*, 1973, **54**, 177. [u] Table 1.

respectively. Negative e^2qQ, with $\eta = 0.7 \pm 0.1$, has also been reported [14] for $[Ph_3Sn(oxin)]$ [structure (II)] (oxin = quinolin-8-olato).

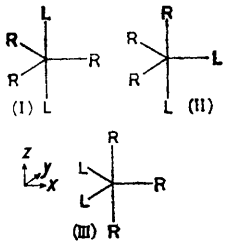

FIGURE 3 Isomers of $[R_3SnL_2]$

Partial Field Gradients due to p *Imbalance.*—The additive model for an e.f.g. at a central atom M bound to ligands L by σ bonds in a closed-shell molecule has been described in detail.[1,2] Associated with each ligand is a partial field gradient parameter [L] defined [1,2,15] in equation (1), where,

$$2e[L] = (1 - R)\langle h_L|v_{zz}|h_L\rangle\sigma_L \quad (1)$$

taking local axes [15] with z directed along the M–L bond, v_{zz} is given by equation (2), R is the Sternheimer factor,

$$v_{zz} = -er^{-5}(3z^2 - r^2) \quad (2)$$

h_L is the appropriate hybrid of metal valence atomic orbitals directed towards the ligand L, and σ_L is an empirical parameter. In the present paper we consider octahedral and trigonal-bipyramidal co-ordination polyhedra in the approximation that the e.f.g. at M arises entirely from imbalance in the metal $5p$ valence shell. The appropriate expressions for h_L and [L] are given in Table 3.

TABLE 3

Partial field gradient (p.f.g.) parameters for p valence electrons in octahedral and trigonal-bipyramidal co-ordination *

Hybrid †	P.f.g. parameter
$h_z^{tba} = (s\cos\theta + p_z + d_{z^2}\sin\theta)/\sqrt{2}$	$[L]^{tba} = -\frac{1}{5}(1 - R)\langle r^{-3}\rangle_p\sigma_L^{tba}$
$h_z^{tbe} = (\sin\theta/\sqrt{3})s + \sqrt{\frac{2}{3}}p_z + (\cos\theta/2\sqrt{3})d_{z^2} - (\cos\theta/\sqrt{2})d_{x^2-y^2}$	$[L]^{tbe} = -\frac{4}{15}(1 - R)\langle r^{-3}\rangle_p\sigma_L^{tbe}$
$h_z^{oct} = (s + \sqrt{3}p_z + \sqrt{2}d_{z^2})/\sqrt{6}$	$[L]^{oct} = -\frac{1}{5}(1 - R)\langle r^{-3}\rangle_p\sigma_L^{oct}$

* tba = trigonal-bipyramidal-apical, tbe = trigonal-bipyramidal-equatorial, oct = octahedral. † Oz directed along metal–ligand axis; θ is s–d mixing parameter (see ref. 1).

The Regression Method.—Let the ^{119}Sn Mössbauer quadrupole splittings $[\frac{1}{2}ce^2qQ(1 + \frac{1}{3}\eta^2)^{\frac{1}{2}}E_\gamma^{-1}$, where c is the velocity of light and the transition energy $E_\gamma = 23.88$ keV] in *trans*-(octahedral)-$[R_2SnL_4]$, *equatorial*-$[R_3SnL_2]$ [(I) in Figure 3], *cis*-$[R_3SnL_2]$ (II), and *mer*-$[R_3SnL_2]$ (III) be denoted Δ_0, Δ_I, Δ_{II}, and Δ_{III}, respectively. By use of Table 3 to calculate Δ_0 and Δ_I, and adding and subtracting a term proportional to σ_R^{tba} to give the correct intercept when R = L, we get equation (3), where m(R,L) and Δ_R are defined in equations (4) and (5) and other symbols have

$$\Delta_I = -m(R,L)\Delta_0 + \Delta_R \quad (3)$$

$$m(R,L) = [(\sigma_R^{tba} - \sigma_L^{tba})/(\sigma_R^{oct} - \sigma_L^{oct})] \quad (4)$$

$$\Delta_R = -\frac{2}{5}ce^2Q(1 - R)\langle r^{-3}\rangle_p E_\gamma^{-1}(\sigma_R^{tba} - \sigma_R^{tbe}) \quad (5)$$

their usual meanings. If R is fixed and L varied then, provided m(R,L) is roughly constant, there should be a linear regression between Δ_I and Δ_0. This is confirmed for the seven (R,L) combinations shown by filled circles in Figure 2, since with L unidentate *X*-ray studies show that structure (I) is adopted.[13] Remembering that since [1] $\sigma_R > \sigma_L$, Δ_0 is positive and Δ_I is negative, the data fit the linear regression given in equation (6) with correlation

$$\Delta_I = -(0.932 \pm 0.092)\Delta_0 + (0.526 \pm 0.397) \text{ mm s}^{-1} \quad (6)$$

coefficient $r = -0.977$ and standard errors as shown. This is a very good correlation; one factor which may have helped is a deliberate attempt to minimize counterion effects by use of the $[BPh_4]^-$ anion in all cationic complexes. However, there is clearly ample reserve for situations where this tactic cannot be used.

It is not surprising that the ratio m(R,L) should be approximately constant, since h_z^{oct} and h_z^{tba} (Table 3) are similar in form, and actually become equal if the parameter θ in h_z^{tba} takes the value 54° 44′.

The intercept at $\Delta_0 = 0$ is the quadrupole splitting of the hypothetical species $[R_5Sn]^-$. However, the extrapolation back to $\Delta_0 = 0$ is a long one, with the result that (as the

[14] J. N. R. Ruddick and J. R. Sams, *J.C.S. Dalton*, 1974, 470.
[15] M. G. Clark, *Mol. Phys.*, 1971, **20**, 257.

standard errors show) the intercept is much more sensitive than the slope to small changes in the data. Thus if the two points with R = Ph are removed, the regression becomes equation (7) with correlation coefficient $r =$

$$\Delta_I = -(0.904 \pm 0.126)\Delta_0 + (0.387 \pm 0.556) \text{ mm s}^{-1} \quad (7)$$

-0.972; a change of only 3% in slope but *ca.* 30% in intercept. In fact the partial field gradients due to Ph and alkyl are distinguishable,[1] and ought ideally to be treated as such when sufficient data are available.

Both Δ_I and Δ_0 have associated with them experimental errors and errors arising from deficiencies in the additive model. The total errors (regarded as pseudo-random) are assumed to be the same for both variables, and the regression lines calculated above (and throughout this paper) are orthogonal mean-square regression lines.[16] Regression procedures based on the assumption that all error is concentrated in one variable only are clearly inappropriate.

Taking axes as shown in Figure 3, the principal components of the e.f.g. tensors [2,17] for structures (II) and (III) are given, in the additive model, by equations (8) to (13).

$$V_{xx}^{II}/e = -[R]^{tba} - \tfrac{1}{2}[R]^{tbe} - [L]^{tba} + 2[L]^{tbe} \quad (8)$$

$$V_{yy}^{II}/e = -[R]^{tba} + \tfrac{5}{2}[R]^{tbe} - [L]^{tba} - [L]^{tbe} \quad (9)$$

$$V_{zz}^{II}/e = 2[R]^{tba} - 2[R]^{tbe} + 2[L]^{tba} - [L]^{tbe} \quad (10)$$

$$V_{xx}^{III}/e = -2[R]^{tba} + 2[R]^{tbe} - \tfrac{1}{2}[L]^{tbe} \quad (11)$$

$$V_{yy}^{III}/e = -2[R]^{tba} - [R]^{tbe} + \tfrac{5}{2}[L]^{tbe} \quad (12)$$

$$V_{zz}^{III}/e = 4[R]^{tba} - [R]^{tbe} - 2[L]^{tbe} \quad (13)$$

Thus, unlike (I) where $\eta = 0$ by symmetry, structures (II) and (III) will, in general, give asymmetric ($\eta \neq 0$) e.f.g.s, with the result that Δ_{II}^2 and Δ_{III}^2 are quadratic functions of Δ_0. However, all available data are such that $|\Delta_0|$ is very much greater than $|\Delta_R|$ and $|\Delta_L|$, where Δ_L, the quadrupole splitting in possibly hypothetical [SnL_5], is given by equation (14). Thus the exact expressions for

$$\Delta_L = -\tfrac{2}{5}ce^2Q(1 - R)\langle r^{-3}\rangle_p E_\gamma^{-1}(\sigma_L^{tba} - \sigma_L^{tbe}) \quad (14)$$

$|\Delta_{II}|$ and $|\Delta_{III}|$, calculated by considering the symmetrized parameter [18] S_{02} and displayed in equations (15*a*) and (16*a*), may be linearized by applying the binomial theorem and neglecting terms of second order in (Δ_R/Δ_0) and (Δ_L/Δ_0) to give equations (15*b*) and (16*b*) [see Appendix (1)]. The

$$|\Delta_{II}| = \tfrac{1}{3}[(\tfrac{13}{4}m\Delta_0)^2 - 8m\Delta_0\Delta_R + 5m\Delta_0\Delta_L + 7\Delta_R^2 - 2\Delta_R\Delta_L + 4\Delta_L^2]^{\frac{1}{2}} \quad (15a)$$

$$= \frac{\sqrt{13}}{6}m(R,L)|\Delta_0| - \frac{8}{3\sqrt{13}}\Delta_R + \frac{5}{3\sqrt{13}}\Delta_L \quad (15b)$$

$$|\Delta_{III}| = \tfrac{1}{3}[7(m\Delta_0)^2 - 2m\Delta_0\Delta_R + 14m\Delta_0\Delta_L + 4\Delta_R^2 - 2\Delta_R\Delta_L + 7\Delta_L^2]^{\frac{1}{2}} \quad (16a)$$

$$= \frac{\sqrt{7}}{3}m(R,L)|\Delta_0| - \frac{1}{3\sqrt{7}}\Delta_R + \frac{\sqrt{7}}{3}\Delta_L \quad (16b)$$

variation in Δ_L with the L encountered in practice is too small to cause noticeable non-linearity in an R-fixed, L-variable regression (see later discussion of Table 9).

Only the magnitudes $|\Delta_{II}|$ and $|\Delta_{III}|$ are considered because the signs of Δ_{II} and Δ_{III} cannot be firmly predicted when η is large, since then only a small change in the relative magnitudes of the principal components of the e.f.g. may cause the principal axes (labelled according to the usual convention [17]) to be permuted, leading to a change in the sign of the e.f.g. Changes of this kind arise, for example, because of distortions from ideal geometry. Thus (see earlier) whereas [Me_3Sn(bipyo)][BPh_4] has e^2qQ negative as predicted by the additive model, both [Ph_3Sn-(bzbz)] and [Ph_3Sn(oxin)] also have negative e^2qQ, contrary to additive-model predictions.

Regression lines for compounds assigned [4] to structure (II) (crosses in Figure 2) and structure (III) (open circles) are given by equations (17) and (18) with correlation co-

$$|\Delta_{II}| = (0.448 \pm 0.058)|\Delta_0| + (0.283 \pm 0.234) \text{ mm s}^{-1} \quad (17)$$

$$|\Delta_{III}| = (0.712 \pm 0.124)|\Delta_0| + (0.868 \pm 0.509) \text{ mm s}^{-1} \quad (18)$$

efficients $r = 0.992$ and 0.914, respectively. If the point (Ph,opo) is excluded from the regression for (III) it becomes equation (19) with $r = 0.881$. From equations (7), (17),

$$|\Delta_{III}| = (0.657 \pm 0.162)|\Delta_0| + (1.103 \pm 0.670) \text{ mm s}^{-1} \quad (19)$$

and (19) the magnitudes of the observed slopes are in the ratio 1 : 0.50 : 0.73 in reasonable agreement with the theoretical values 1 : 0.60 : 0.88 given by equations (3), (15), and (16).

As already mentioned, the values for the intercepts at $\Delta_0 = 0$ are rather less accurate than the slopes. Nevertheless, the regressions for (I) and (III) clearly imply that both Δ_R and Δ_L are positive (V_{zz} negative). In the case of Δ_L this is contrary to previously held opinion [5,19] that $\Delta(SnCl_5^-)$ would prove to be negative. [Unfortunately, an attempt [5] to determine the sign of $\Delta(SnCl_5^-)$ by comparing $^{119}SnCl_5^-$ and $^{121}SbCl_5$ is invalidated by the phase change in the latter compound.[20]] However, p.q.s. values deduced on the assumption that Δ_L is positive lead to a consistent interpretation of ^{119}Sn quadrupole coupling constants.

Tolerance Limits.—If it is assumed that the discrepancies between additive-model predictions and actual quadrupole splittings vary randomly from compound to compound, then the validity of conclusions based on application of the additive model can be quantitatively investigated by use of tolerance limits. The method is generally applicable, although we illustrate it only in the context of trigonal-bipyramidal geometry. However, the assumption that discrepancies are pseudo-random should not be made lightly; for example, in tetrahedral structures there are systematic differences between the $ASnX_3$ and A_2SnX_2 systems which cannot be accounted for by an additive model based on ideal tetrahedral geometry.[8] This suggests that a data base is most likely to be pseudo-random if it gives roughly equal weight to a number of different structures.

Associated with each regression line is a population standard error *s*, measuring the scatter of data points by the root-mean-square of their (signed) perpendicular

[16] H. Cramér, 'Mathematical Methods of Statistics,' University Press, Princeton, 1946, sect. 21.6.

[17] For basic theory of e.f.g. tensors see M. H. Cohen and F. Reif, *Solid-State Phys.*, 1957, **5**, 321.

[18] M. G. Clark, *J. Chem. Phys.*, 1971, **54**, 697.

[19] R. V. Parish and R. H. Platt, *Inorg. Chim. Acta*, 1970, **4**, 65.

[20] R. F. Schneider and J. V. Di Lorenzo, *J. Chem. Phys.*, 1967, **47**, 2343.

distances from the line. For a line $y = mx + c$, based on n data points (x_i, y_i), s may be estimated by equation (20), where $[dd]$ is defined in equation (21). The (parallel-

$$s^2 = [dd]/(n - 2)(1 + m^2) \quad (20)$$

$$[dd] = \sum_{i=1}^{n} (y_i - mx_i - c)^2 \quad (21)$$

displacement) tolerance limits are lines parallel to the regression line lying on each side of it at distances of [21] $\pm s(1 + n^{-1})^{\frac{1}{2}} t(P, n - 2)$, where $t(P, n - 2)$ denotes the t-distribution P-percentage point on $(n - 2)$ degrees of freedom. The probability that an additional observation, properly belonging to the regression, will lie outside the tolerance limits is $< P/100$. For the values of n usually encountered in practice it is convenient to use limits of $\pm 3s$, which will correspond to a P of between 5% and 2%, or over 2 units of support in likelihood terms.[22]

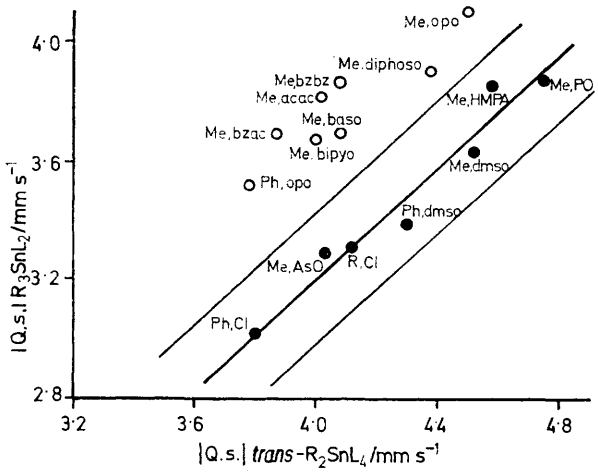

FIGURE 4 Regression line for data on structure (I) (filled circles) replotted with tolerance limits described in text. Open circles show data for structure (III)

The values of s estimated for equations (6), (17), and (18) are 0.05, 0.05, and 0.06 mm s^{-1}. In Figure 4 the data points (filled circles), regression line, and $\pm 3s$ tolerance limits for structure (I) are shown together with the data points (open circles) for structure (III). All the latter points lie outside the limits for (I). Further, if we were to assume in advance that the open circles all belonged to the same unknown isomer of R_3SnL_2, our belief that this isomer was not (I) would be stronger still, since the tolerance limits for the mean of the perpendicular displacements are given by dividing the one-point tolerance limits by $\sqrt{N}$, where N (= 8 in the present case) is the number of points being jointly tested [see Appendix (2)]. This is one example of the general point that tolerance limits can be adjusted to take into account other evidence or preconceptions. The method of likelihood is particularly useful in this context, and for this reason has been illustrated in Appendix (2).

Partial Quadrupole Splitting Parameters for $^{119}Sn^{IV}$.—The quantities [L] in Table 3 are not susceptible to direct experimental determination.[1] Actual p.q.s. scales may be based on measurements of either [Scheme (*A*)] equations (22) and (23) or [Scheme (*B*)] equations (24) and (25),

$$\{L\}^{tba} = \tfrac{1}{2}ce^2|Q|E_\gamma^{-1}([L]^{tba} - [X]^{tba}) \quad (22)$$

$$\{L\}^{tbe} = \tfrac{1}{2}ce^2|Q|E_\gamma^{-1}([L]^{tbe} - \tfrac{4}{3}[X]^{tba}) \quad (23)$$

$$\{L\}^{tba} = \tfrac{1}{2}ce^2|Q|E_\gamma^{-1}([L]^{tba} - \tfrac{3}{4}[X]^{tbe}) \quad (24)$$

$$\{L\}^{tbe} = \tfrac{1}{2}ce^2|Q|E_\gamma^{-1}([L]^{tbe} - [X]^{tbe}) \quad (25)$$

where X is a fixed reference ligand. An arbitrary assumption that [7] $[X]^{tba} = 0$ is equivalent to Scheme (*A*), while an assumption that $[X]^{tbe} = 0$ is equivalent to Scheme (*B*). In agreement with ref. 7, we favour Scheme (*A*) with X = Cl or Br.

The importance of establishing representative p.q.s. values for the key frequently occurring alkyl, phenyl, and halogen ligands has already been emphasized.[1] Since $\{X\}^{tba} = \{Cl\}^{tba} = \{Br\}^{tba} = 0$ by definition, we have to determine values of $\{R\}^{tba}$, $\{R\}^{tbe}$ (R = alkyl and Ph), and $\{X\}^{tbe}$. Mössbauer data are available for $[(alkyl)_nSnX_{5-n}]$ with n = 0, 1, 2, and 3. In all cases the alkyl groups occupy equatorial positions.[13] Thus good representative values for $\{alkyl\}^{tbe}$ and $\{X\}^{tbe}$, together with 'errors' measuring the discrepancies between theory and observation, may be obtained by calculating the best least-squares solution of equations (26) to (29). The left-hand sides of these equations are additive-model predictions for minus

$$-3\{R\}^{tbe} = +3.39 \quad (26)$$

$$\sqrt{7}\{R\}^{tbe} - \frac{1}{\sqrt{7}}\{X\}^{tbe} = -3.45 \quad (27)$$

$$2\{R\}^{tbe} - \tfrac{1}{2}\{X\}^{tbe} = -1.82 \quad (28)$$

$$-3\{X\}^{tbe} = -0.63 \quad (29)$$

the quadrupole splittings (Q is negative) in $R_3SnX_2^-$, $R_2SnX_3^-$, $RSnX_4^-$, and SnX_5^-, respectively, linearized if $\eta \neq 0$ by neglecting terms of second order in $\{X\}^{tbe}/\{R\}^{tbe}$. The right hand sides are unweighted averages in units of mm s^{-1} of all literature values available to us,[19,23,24] with the sign (of V_{zz}) for SnX_5^- chosen negative following the regression analysis.

The least squares solutions [25] of equations (26)—(29) are $\{R\}^{tbe} = -1.13 \pm 0.11$ mm s^{-1} and $\{X\}^{tbe} = +0.20 \pm 0.15$ mm s^{-1}. The standard errors indicate that the rough tolerance limit of 0.4 mm s^{-1} suggested [1] for application of the additive model to tetrahedral and octahedral organotin(IV) compounds is suitable for trigonal bipyramidal systems too. Note that the estimates of $\{R\}^{tbe}$ and $\{X\}^{tbe}$ are not statistically independent [in fact, $(\text{covariance})^{\frac{1}{2}} = 0.05$ mm s^{-1}], although the correlation coefficient $r = 0.15$ is quite small. Since our procedure pools data from four different stoicheiometries it should minimize the effect of any bias of the type exemplified [8] by the $[ASnX_3]$ and $[A_2SnX_2]$ systems already mentioned; instead the effects of distortions from ideal geometry are reflected in the standard errors obtained.

Next, we derive additive-model expressions for Δ_{II} and

[21] N. Arley and K. R. Buch, 'Probability and Statistics,' Chapman and Hall, London, 1950, sect. 11.8.
[22] A. W. F. Edwards, 'Likelihood,' University Press, Cambridge, 1972, sect. 9.5.
[23] R. V. Parish and C. E. Johnson, *J. Chem. Soc.* (*A*), 1971, 1906.
[24] N. W. G. Debye, E. Rosenberg, and J. J. Zuckerman, *J. Amer. Chem. Soc.*, 1968, **90**, 3234.
[25] J. Topping, 'Errors of Observation and their Treatment,' Inst. Phys. and Phys. Soc., London, 1962, sects. 44 and 45; ref. 21, sects. 12.6 and 12.7.

Δ_{III} (R_3SnL_2 compounds) and Δ_I for [R_3SnLL'] compounds. The required expressions * are given in equations (30) to (32), where equations (31) and (32) are linearized under the same approximations as equations (15*b*) and (16*b*).

$$|\Delta_I(R_3SnLL')| = |2\{L\}^{tba} + 2\{L'\}^{tba} - 3\{R\}^{tbe}| \quad (30)$$

$$|\Delta_{III}(R_3SnL_2)| = [16\{R\}^{tba\,2} - 8\{R\}^{tba}\{R\}^{tbe} - 16\{R\}^{tba}\{L\}^{tbe} + 4\{R\}^{tbe\,2} - 2\{R\}^{tbe}\{L\}^{tbe} + 7\{L\}^{tbe\,2}]^{\frac{1}{2}}$$
$$\approx [-8\{R\}^{tba} - \{R\}^{tbe} + 7\{L\}^{tbe}]/\sqrt{7} \quad (31)$$

$$|\Delta_{II}(R_3SnL_2)| = [4\{R\}^{tba\,2} - 8\{R\}^{tba}\{R\}^{tbe} + 8\{R\}^{tba}\{L\}^{tba} - 4\{R\}^{tba}\{L\}^{tbe} + 7\{R\}^{tbe\,2} - 8\{R\}^{tbe}\{L\}^{tba} - 2\{R\}^{tbe}\{L\}^{tbe} + 4\{L\}^{tba\,2} - 4\{L\}^{tba}\{L\}^{tbe} + 4\{L\}^{tbe\,2}]^{\frac{1}{2}}$$
$$\approx [2\{R\}^{tba} - 8\{R\}^{tbe} + 2\{L\}^{tba} + 5\{L\}^{tbe}]/\sqrt{13} \quad (32)$$

A value for $\{R\}^{tba}$ may now be calculated by use of equation (31), the previously derived values of $\{R\}^{tbe}$ and $\{X\}^{tbe}$, and an estimate of the quadrupole splitting in hypothetical *mer*-[R_3SnX_2] obtained by interpolating in the regression of Δ_{III} against Δ_0 at $\Delta_0 = +4.12$ mm s^{-1}, the averaged value [1] for *trans*-[R_2SnX_4]. The interpolation gives $|\Delta_{III}(R_3SnX_2)| = 3.80$ mm s^{-1}. Since the point concerned lies near the centre of gravity of the data on structure (III) (Figure 2) the interpolated value is virtually independent of the choice of data base, giving confidence that the estimate $\{R\}^{tba} = -0.94 \pm 0.13$ mm s^{-1} obtained from this quadrupole splitting and equation (31) is a good representative value of $\{R\}^{tba}$. The error quoted reflects only the variance–covariance values given above for $\{R\}^{tbe}$ and $\{X\}^{tbe}$. It is encouraging to note that the value of $\{R\}^{tba}$ calculated from $m(R,X) = (\{R\}^{tba}/\{R\}^{oct}) = +0.904$ [see equations (4) and (7)] is -0.93 mm s^{-1}.

The available data on phenyl derivatives are more limited. The average of the ^{119}Sn quadrupole splittings [19,26] in [NMe_4][Ph_3SnCl_2] and [$Ph_3PC_{10}H_{21}$][Ph_3SnCl_2] [both structure (I)] gives $\{Ph\}^{tbe} = -0.98$ mm s^{-1}. Interpolation in the regression of Δ_{III} against Δ_0, as already described, gives $\{Ph\}^{tba} = -0.89$ mm s^{-1}. There is not sufficient evidence for 'errors' to be assigned to these values individually, but the foregoing discussion indicates that *ca.* 0.15 mm s^{-1} would be a sensible guess.

Notice that our values for $\{R\}^{tbe}$ and $\{R\}^{tba}$, and the positive quadrupole splitting for [R_5Sn]$^-$, are consistent with theoretical predictions. The theoretical ratio of $\{R\}^{tba}/\{R\}^{tbe}$ is equal to $\frac{3}{4}[(\sigma_R{}^{tba} - \sigma_X{}^{tba})/(\sigma_R{}^{tbe} - \sigma_X{}^{tba})]$ (Table 3), compared to our calculated values of 0.83 for R = alkyl and 0.91 for R = Ph. Since previous results [1] indicate that $(\sigma_R{}^{tet} - \sigma_X{}^{tet})$ is within *ca.* 12% of $(\sigma_R{}^{oct} - \sigma_X{}^{oct})$, we expect that $[(\sigma_R{}^{tba} - \sigma_X{}^{tba})/(\sigma_R{}^{tbe} - \sigma_X{}^{tba})] \approx 1$ and $(\{R\}^{tba}/\{R\}^{tbe}) \approx 0.75$. Thus our values of 0.83 and 0.91 seem entirely reasonable. If [7] $(\{R\}^{tba}/\{R\}^{tbe}) > 1$, then $(\sigma_R{}^{tba} - \sigma_X{}^{tba})$ would have to be more than 33% greater than $(\sigma_R{}^{tbe} - \sigma_X{}^{tba})$, and this does not appear likely. Our values for $\{R\}^{tba}/\{R\}^{tbe}$ imply that $\Delta(R_5Sn^-) > 0$, whereas $\Delta(R_5Sn^-)$ negative would require $0.75 > (\{R\}^{tba}/\{R\}^{tbe}) \gtrsim 0.5$, which is not consistent with our results.

Available experimental data are such that p.q.s. parameters for other ligands L must be derived by *ad hoc* procedures based on one or two compounds believed to be reasonably close to ideal geometry. We have calculated values for ligands commonly occurring in five-co-ordination by use of quadrupole splittings observed (Table 2) in either [R_3SnL_2] (*equatorial*, *cis*, or *mer*) or *equatorial*-[R_3SnLL']. For *equatorial* (I) and *mer* (III) isomers $\{L\}^{tba}$ and $\{L\}^{tbe}$, respectively, are readily obtained by equating the observed splittings to the additive model expressions given in equations (30) and (31). The *cis*-isomer (II) [equation (32)] yields either $\{L\}^{tba}$ or $\{L\}^{tbe}$ if the other is known. However, since the coefficient of $\{L\}^{tba}$ in the last part of equation (32) is rather small, any error in $|\Delta_{II}|$ will be magnified, and [assuming isomer (I) is not available] it is preferable to determine $\{L\}^{tba}$ from Δ_I[R_3SnL_2] obtained by interpolation into the regression of Δ_I against Δ_0 at the measured value of Δ_0(*trans*-[R_2SnL_4]) [or twice $|\Delta$(*cis*-R_2SnL_4)$|$, if necessary]. Indeed, this is the only method for bidentate chelates L_2 not available in both *cis*- and *mer*-structures.

Apical parameters for all chelates listed in Table 4 were obtained by this interpolation procedure. For example, the value $\Delta_0 = +4.02$ mm s^{-1} for *trans*-[$Me_2Sn(acac)_2$] [Table 2, compound (12)] was inserted into equation (7) to give $\Delta_I = -3.25$ mm s^{-1} for hypothetical *equatorial*-[$Me_3Sn(acac)$], and $\{acac\}^{tba}$ was then calculated by use of equation (30). The other values listed were obtained in a similar way, taking $\Delta_0 = 2|\Delta$[*cis*-oct.-$(alkyl)_2Sn(oxin)_2$]$|$ in the case of oxin. Equatorial parameters were obtained by use of equation (31), or (for oxin only) equation (32), and data from Table 2 as noted. The remaining unidentate ligands are generally found only in the apical position, and values of $\{L\}^{tba}$ were obtained by applying equation (30) to the compounds noted. If required, equatorial parameters for these ligands could be estimated by transforming from Δ_I to Δ_{III}, or by use of equation (41) discussed later.

Since the differences $(\{R\}^{tba} - \{R\}^{tbe})$ and $(\{X\}^{tba} - \{X\}^{tbe})$ are only 1.4 and 1.33 standard errors, respectively, it is important to point out that by equations (22) and (23) $\{L\}^{tba} = \{L\}^{tbe}$ would only imply $[L]^{tba} = [L]^{tbe} = [L]$ if $[X] = 0$, which manifestly could not be true since SnX_5^- has a quadrupole splitting of 0.63 mm s^{-1}. If $[L]^{tba}$ were equal to $[L]^{tbe}$ then from equations (22) and (23) ($\{L\}^{tba}$ in $\{L\}^{tbe}$) would be constant. In fact, for those ligands — Table 4 where both parameters are available, the difference ranges from -0.24 to $+0.19$ mm s^{-1}. As discussed in the next section (see Table 7) the chemically significant quantity is actually $(3\{L\}^{tbe} - 4\{L\}^{tba})$.

Note that the ordering of $-\{L\}^{tba}$ ($\propto \sigma_L{}^{tba}$) values is very close to that observed [1,3,6] for $-\{L\}^{oct}$:

oct: R > Ph > I > py > pyO ~ Ph_3AsO > pip ~ Cl > dmf > NCS > dmso ~ hmpa > Ph_3PO

tba: R > Ph > I > py ~ Ph_3AsO ~ pyO ~ Cl ~ pip > NCS ~ dmso > Ph_3PO ~ dmf ~ hmpa

where ~ denotes differences in p.q.s. of <0.03 mm s^{-1}. This indicates that the donor strength of common ligands (as measured by σ_L) behaves consistently in trigonal-bipyramidal-apical and octahedral co-ordination, and

* Exact expressions were obtained by calculating the symmetrized parameter S_{02} (ref. 18) and linearized approximations follow by expansion (Appendix 1). A useful check on the linearized expressions follows from equations (22) and (23): the algebraic sum of the coefficients of $\{\ \}^{tba}$ terms and $\frac{4}{3}$ × coefficients of $\{\ \}^{tbe}$ terms must be zero, provided that if apical X is present $\{X\}^{tba}$ must be explicitly included in the expression even though $\{X\}^{tba} \equiv 0$.

[26] J. Ensling, Ph. Gütlich, K. M. Hassellbach, and B. W. Fitzsimmons, *J. Chem. Soc.* (*A*), 1971, 1940.

TABLE 4

Estimated partial quadrupole splitting parameters for trigonal-bipyramidal organotin(IV) compounds

Ligand *	$\{L\}^{tba}$ †/ mm s^{-1}	Data used ‡	$\{L\}^{tbe}$ †/ mm s^{-1}	Data used ‡
Cl, Br	0	*a*	+0.20	*b*
alkyl	−0.94	*b*	−1.13	*b*
Ph	−0.89	*b*	−0.98	*b*
oxin	−0.05 §	(19)	+0.04	(201)
acac	−0.03 §	(12)	+0.20	(305)
bzac	−0.07 §	(14)	+0.15	(307)
bzbz	−0.02 §	(13)	+0.22	(306)
opo	+0.075 §	(8)	+0.31	(301)
diphoso	+0.05 §	(9)	+0.24	(302)
baso	−0.02 §	(10)	+0.16	(303)
bipyo	−0.04 §	(11)	+0.15	(304)
Ph_3PO	+0.12	(101)		
Ph_3AsO	−0.02	(105)		
hmpa	+0.13	(102), (108)		
dmso	+0.09	(103), (106)		
dmf	+0.13	(109)		
dma	+0.16	(111)		
py	−0.035	(112), (113)		
pyO	0.00	(114)		
NCS	+0.065	(115)		
F	+0.11	(116)		
I	−0.08	(117)		
OH	−0.13	(118)		
H_2O	+0.18	(110)		
N_3	+0.03	(120)		
pip	+0.01	(135)		
CN	−0.065	(119)		
NO_2R	0.00	(134)		
NO_3	+0.11	(121), (122)		
O·CO·H	+0.04	(131)		
OAc	+0.075	(123)		
$O{\cdot}CO{\cdot}CH_2I$	+0.11	(124)		
$O{\cdot}CO{\cdot}CH_2Br$	+0.13	(125)		
$O{\cdot}CO{\cdot}CH_2Cl$	+0.13	(126)		
$O{\cdot}CO{\cdot}CBr_3$	+0.19	(127)		
$O{\cdot}CO{\cdot}CCl_3$	+0.19	(128)		
$O{\cdot}CO{\cdot}CHCl_2$	+0.175	(129)		
$O{\cdot}CO{\cdot}CF_3$	+0.21	(130)		
SO_3CF_3	+0.30	(132)		
SO_3Me	+0.21	(133)		

[a] By definition. [b] See text.

* For abbreviations see footnotes to Tables 1 and 2. † $\{L\}^{tba}$ and $\{L\}^{tbe}$ are defined in equations (22) and (23). All values may be assigned nominal standard errors of *ca.* 0.15 mm s^{-1}. ‡ Code numbers refer to Table 2. § Calc. after interpolation into equation (7) with data from compounds noted; see text for details.

further confirms the assumption concerning the comparability of oct and tba bonds made in our discussion of the regression method.

The p.q.s. parameters in Table 4 depend on the theoretical analysis of the regression lines (Figure 2) only for the qualitative conclusion that Δ_R and Δ_L are both positive. [Interpolation into the regression of $|\Delta_{III}|$ against $|\Delta_0|$ does not depend on the interpretation of this regression by equation (16).] Thus quantitative comparison of the observed slopes and intercepts with predictions calculated from the p.q.s. parameters in Table 4 gives an indication of the accuracy with which equations (3), (15), and (16) describe the regressions displayed in Figure 2. The results are shown in Table 5, together with values calculated on the assumptions $[L]^{tba} \equiv [L]^{tbe}$, $\Delta(SnX_5^-) > 0$ and $[L]^{tba} \equiv [L]^{tbe}$, $\Delta(SnX_5^-) < 0$. Notice that all values calculated from Table 4 agree with the observed parameters to well within experimental error, whereas neither of the cases with $[L]^{tba} \equiv [L]^{tbe}$ gives good agreement for all six parameters. Further, when the p.q.s. parameters from Table 4 are used the directions of changes in intercepts on including phenyl compounds [equations (6) and (18)] are predicted correctly, since the calculated Δ_{Ph} (= +0.62 mm s^{-1}) is larger than Δ_{alkyl}. The calculated values of m(alkyl,X) = 0.92 and m(Ph,X) 0.93 are virtually identical.

DISCUSSION

Application of $^{119}Sn^{IV}$ *Parameters.*—In Table 6 the quadrupole splittings observed in a selection of $[R_3SnL_2]$, $[R_3SnLL']$, and $[R_2SnL_2L']$ species are compared with predictions calculated by use of the parameters given in Table 4. The structural assignments noted are based on the agreement between predicted and observed values, and in many cases are supported by the systematics of organotin(IV) structural chemistry.[13] Only $[Me_3SnpyNO_3]$ [compound (11)] shows a discrepancy greater than the tolerance limit of 0.4 mm s^{-1}, indicating that the tin atom in this compound is not five-co-ordinate.

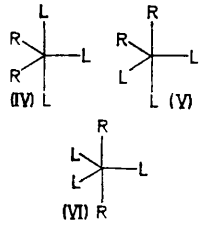

FIGURE 5 Isomers of $[R_2SnL_3]$

The three isomers of $[R_2SnL_3]$ (Figure 5) are often readily distinguished when $\{L\}/\{R\}$ is small, since then for given R and L we have from equations (33) to (35)

$$|\Delta_{IV}| \approx (-7\{R\}^{tbe} + 8\{L\}^{tba} + \{L\}^{tbe})/\sqrt{7} \quad (33)$$

$$|\Delta_{V}| \approx (-2\{R\}^{tba} - 5\{R\}^{tbe} - 2\{L\}^{tba} + 8\{L\}^{tbe})/\sqrt{13} \quad (34)$$

$$|\Delta_{VI}| = -4\{R\}^{tba} + 3\{L\}^{tbe} \quad (35)$$

that $|\Delta_{VI}| > |\Delta_{IV}| > |\Delta_{V}|$ with differences $\geqslant$0.4 mm s^{-1}.

TABLE 5

Comparison of slope (col. *A*) and intercept (col. *B*) of observed regression lines with values calculated on various assumptions

	Eq. (7)		Eq. (17)		Eq. (19)	
	A	*B* *	*A*	*B* *	*A*	*B* *
Obs.	−0.90 ±0.13	0.39 ±0.56	0.45 ±0.06	0.28 ±0.23	0.66 ±0.16	1.10 ±0.67
From Table 4	−0.92	0.37	0.56	−0.18	0.81	0.47
$[L]^{tba} \equiv [L]^{tbe}$, $\Delta_X > 0$	−1.30	1.97	0.75	−1.05	1.15	0.31
$[L]^{tba} \equiv [L]^{tbe}$, $\Delta_X < 0$	−0.89	0.29	0.49	−0.39	0.79	−0.59

* Units mm s^{-1}.

For example, if R = alkyl and L = Cl, $|\Delta_{VI}| = 4.36$ mm s^{-1}, $|\Delta_{IV}| = 3.07$ mm s^{-1}, $|\Delta_{V}| = 2.53$ mm s^{-1}. In Table 6 the agreement between observed and predicted quadrupole splittings strongly suggests that compounds (33)—(41) have structure (IV). With $\{L'\} \neq \{L\}$ in $[R_2SnL_2L']$, structures (IV) and (V) have two isomers, namely L′ apical [(IVa) and (Va)] and L′ equatorial [(IVb) and (Vb)]. The expressions corresponding to equation (33) are equations (36) and (37), although, as

$$|\Delta_{IVa}| \approx -\sqrt{7}\{R\}^{tbe} + (4\{L'\}^{tba} + 4\{L\}^{tba} + \{L\}^{tbe})\sqrt{7} \quad (36)$$

$$|\Delta_{IVb}| \approx -\sqrt{7}\{R\}^{tbe} + (8\{L\}^{tba} + \{L'\}^{tbe})\sqrt{7} \quad (37)$$

noted in Table 6, the quadrupole splittings of the two structures are scarcely distinguishable.

Compounds (32) and (33) in Table 6 illustrate the unreliability (already noted) of additive-model predictions of sign. Here, as in *cis*-octahedral systems,[23] the discrepancies may be attributed to distortions from ideal geometry.[14]

When compound (11) is excluded the agreement in Table 6 is generally very good, the observed and calculated values of |q.s.| having a correlation coefficient $r = 0.94$. The agreement may be further tested by examining the quantities $\bar{x} = \Sigma x/n$, $s = [\Sigma(x - \bar{x})^2/(n - 1)]^{\frac{1}{2}}$, and [27] t, where t and x are defined in equations

TABLE 6

Obs. and calc. quadrupole splittings for some organotin-(IV) compounds

Compound †	Obs. q.s. ‡	Calc. q.s. §
(i) Structure (I) *		
(1) [$Me_3SnCl(dma)$] [a]	3.69	−3.69
(2) [$Me_3SnCl(hmpa)$] [a]	3.52	−3.65
(3) [$Me_3SnCl(pmpo)$] [a]	3.45	−3.38
(4) [$Me_3SnCl(Ph_3PO)$] [a]	3.49	−3.63
(5) [$Me_3SnNCS\{(pip)_3PO\}$] [b]	3.82	−3.77
(6) [$Me_3SnBr\{(morph)_3PO\}$] [b]	3.63	−3.64
(7) [$Me_3SnBr(quinoline)$] [c]	3.20	−3.31
(8) [Me_3SnCl] [d]	3.44	−3.39
(9) [Me_3SnNO_3] [f]	4.14	−3.82
(10) [$(Me_3Sn)_2(OH)N_3$] [e]	3.25	−3.18
(11) [$Me_3SnpyNO_3$] [f]	4.20	−3.52 ¶
(12) [$Ph_3SnCl(dmso)$] [b]	3.19	−3.11
(13) [$Ph_3SnBr(Ph_3PO)$] [b]	3.20	−3.18
(14) [$Ph_3SnBr(dmso)$] [b]	3.22	−3.11
(15) [$Ph_3SnCl(Ph_3PO)$] [b]	3.23	−3.18
(16) [$Ph_3SnNCS(dmso)$] [b]	3.33	−3.24
(17) [Ph_3SnNCS] [b]	3.54	−3.19
(18) [$Ph_3SnNCS(Ph_3PO)$] [b]	3.48	−3.30
(19) [$Ph_3Sn(OAc)$] [g,o]	3.32	−3.23
(20) [$Ph_3Sn(OCOCH_2I)$] [g]	3.59	−3.38
(21) [$Ph_3Sn(OCOCH_2Cl)$] [g,o]	3.50	−3.45
(22) [$Ph_3Sn(OCOCH_2Br)$] [g]	3.51	−3.45
(23) [$Ph_3Sn(OCOCHCl_2)$] [g,o]	3.77	−3.63
(24) [$Ph_3Sn(OCOCCl_3)$] [g]	3.97	−3.69
(25) [$Ph_3Sn(OCOCF_3)$] [g]	4.00	−3.77
(26) [Ph_3SnF] [d]	3.58	−3.37
(27) [Ph_3SnOH] [d]	2.73	−2.41
(28) [Ph_3SnN_3] [d]	3.19	−3.05
(29) [$Ph_3SnCl(Ph_3AsO)$] [p]	3.09	−2.89
(ii) Structure (III)		
(30) [$Ph_3Sn(opo)$][BPh_4] [h]	3.52	−3.88
(31) [$Ph_3Sn(diphoso)$][BPh_4] [h]	3.56	−3.70
(iii) Structure (II)		
(32) [$Ph_3Sn(bzbz)$] [i]	−2.25	+1.98

TABLE 6 (*Continued*)

Compound † (iv) Structure (IV)	Obs.q.s. ‡	Calc.q.s. §
(33) [$(alkyl)_2SnCl(oxin)$] [j,q]	−3.12	+2.92
(34) [$Et_2SnI(oxin)$] [j]	2.85	+2.80
(35) [$Et_2SnNCS(oxin)$] [j]	3.07	+3.02
(36) [$Ph_2SnCl(oxin)$] [j,q]	+2.40	+2.53
(37) [NEt_4][Ph_2SnCl_3] [k]	2.62	+2.59
(38) [$Ph_2SnCl_2(Ph_3PO)$] [l]	2.98	+2.77 **
(39) [$Ph_2SnCl_2(Ph_3AsO)$] [l]	2.83	+2.57 ††
(40) [$Ph_2SnCl(bzbz)$] [m]	2.61	+2.65
(41) [$Ph_2SnCl_2\{(alkyl)_2SO\}$] [n]	3.05	+2.73 **

* See Figures 3 and 5. † pmpo = *p*-Methylpyridine *N*-oxide; morph = morpholino; for other abbreviations see Tables 1 and 2. ‡ $\frac{1}{2}ce^2qQ(1 + \frac{1}{3}\eta^2)^{\frac{1}{2}}E_\gamma^{-1}$ in mm s^{-1}. Values are unweighted averages, where appropriate, of measurements at or <80 K. Signs are explicitly stated only when an experimental determination is known to us. § Calc. for structure noted by use of the parameters in Table 4, with the additional assumptions: $\{pmpo\}^{tba} = \{pyO\}^{tba}$, $\{(pip)_3PO\}^{tba} = \{hmpa\}^{tba} = \{(morph)_3PO\}^{tba}$, $\{quinoline\}^{tba} = \{py\}^{tba}$, and $\{(alkyl)_2SO\}^{tba} = \{dmso\}^{tba}$. ¶ Discrepancy between observed and calculated values indicates that compound is not trigonal-bipyramidal. ** Apical Ph_3PO and $(alkyl)_2SO$ give slightly better fit than equatorial. †† Apical and equatorial Ph_3AsO indistinguishable.

[a] J. C. Hill, R. S. Drago, and R. H. Herber, *J. Amer. Chem. Soc.*, 1969, **91**, 1644. [b] Ref. 26. [c] J. Nasielski, N. Sprecher, J. de Vooght, and S. Lejeune, *J. Organometallic Chem.*, 1967, **8**, 97. [d] Mean of values collected in ref. 3. [e] N. Bertazzi, G. Alonzo, R. Barbieri, and R. H. Herber, *J. Organometallic Chem.*, 1974, **65**, 23. [f] D. Potts, H. D. Sharma, A. J. Carty, and A. Walker, *Inorg. Chem.*, 1974, **13**, 1205. [g] B. F. E. Ford and J. R. Sams, *J. Organometallic Chem.*, 1971, **31**, 47. [h] This work. [i] Ref. 12. [j] R. C. Poller and J. N. R. Ruddick, *J. Chem. Soc.* (*A*), 1969, 2273. [k] Ref. 24. [l] F. P. Mullins, *Canad. J. Chem.*, 1971, **49**, 2719. [m] G. M. Bancroft and T. K. Sham, unpublished work. [n] R. S. Randell, R. W. J. Wedd, and J. R. Sams, *J. Organometallic Chem.*, 1971, **30**, *C*19. [o] Mean of values collected by P. J. Smith, *Organometallic Chem. Rev. A*, 1970, **5**, 373. [p] R. W. J. Wedd and J. R. Sams, *Canad. J. Chem.*, 1970, **48**, 71. [q] Ref. 14.

(38) and (39) and the number of values of x is n. For the data in Table 6 [(11) excluded] $n = 40$, $\bar{x} = 0.092$

$$t = n^{\frac{1}{2}}\bar{x}/s \quad (38)$$

$$x = (|\text{obs. q.s.}| - |\text{calc. q.s.}|) \quad (39)$$

mm s^{-1}, $s = 0.154$ mm s^{-1}, and $t = 3.8$. The value of s confirms the good agreement, and the suggestion of 0.4 mm s^{-1} as a crude tolerance limit for one observation. However, the value of $\bar{x}$ suggests that the calculated magnitudes tend to underestimate very slightly the observed ones, and this is confirmed by the t test, since the probability of $|t| \geqslant 3.8$ occurring by chance is slightly <0.1%. If this observation of bias is confirmed in further applications a slight revision of the parameters in Table 4 may be advisable. In particular the p.q.s. parameters for Ph were based on rather limited data, yet $\{Ph\}^{tbe}$ especially is quite severely tested in Table 6 since many of the compounds contain this ligand in an equatorial position.

It is of interest to compare the performance of the parameters in Table 4 with p.q.s. parameters calculated on the simpler assumption, used in pioneering work,[19] that apical and equatorial ligands may be assigned the same partial field gradient parameter. In cases where

[27] Ref. 21, sect. 11.14.

ligands appear only in one kind of position, *i.e.* compounds with structure (I), the assumption of a single partial field gradient parameter, although open to the theoretical objections discussed, will be empirically satisfactory; the test comes with compounds (30) to (41) where the same ligand occurs at both apical and equatorial sites. Thus we have calculated the p.q.s. parameters required for calculation of these quadrupole splittings on the assumption that $[L]^{tba} \equiv [L]^{tbe}$ both for $\Delta(SnX_5^-) > 0$ and (to test further our conclusion on this question) for $\Delta(SnX_5^-) < 0$. Comparing observed and calculated values for the twelve compounds we get the following values for s and $\bar{x}$:

(i) Parameters from Table 4: $s = 0.202$ mm s^{-1}, $\bar{x} = +0.067$ mm s^{-1}

(ii) $[L]^{tba} \equiv [L]^{tbe}$ and $\Delta(SnX_5^-) > 0$: $s = 0.319$ mm s^{-1}, $\bar{x} = +0.352$ mm s^{-1}

(iii) $[L]^{tba} \equiv [L]^{tbe}$ and $\Delta(SnX_5^-) < 0$: $s = 0.321$ mm s^{-1}, $\bar{x} = -0.067$ mm s^{-1}

Examination by the Snedecor F test shows that the standard error, s, for (i) is significantly smaller than either of the others at a 7% level, *i.e.* the probability of variance ratios equal to or greater than the observed values is only 0.07. Also, whereas for assumptions (i) all values of $|x|$ are <0.4 mm s^{-1}, there are five cases where $|x| \geqslant 0.4$ mm s^{-1} for (ii), and two for assumptions (iii). In addition $\bar{x}$ shows that assumptions (ii) give unacceptably large bias. Thus, apart from the arguments given, even at a purely empirical level the use of distinct apical and equatorial partial field gradient parameters gives a significantly better description of quadrupole splittings.

In considering those ligands for which both $\{L\}^{tba}$ and $\{L\}^{tbe}$ are available it is important to realize [1] that

TABLE 7

Values of $(3\{L\}^{tbe} - 4\{L\}^{tba})$ calc. from Table 4

Ligand *	$(3\{L\}^{tbe} - 4\{L\}^{tba})$ †/ mm s^{-1}
Cl, Br	+0.60
alkyl	+0.37
Ph	+0.62
oxin	+0.32
acac	+0.72
bzac	+0.73
bzbz	+0.74
opo	+0.63
diphoso	+0.52
baso	+0.56
bipyo	+0.61

* For abbreviations see footnotes to Tables 1 and 2. † $(3\{L\}^{tbe} - 4\{L\}^{tba}) = \frac{2}{5}ce^2|Q|E_\gamma^{-1}(1 - R)\langle r^{-3}\rangle_p(\sigma_L^{tba} - \sigma_L^{tbe}) = \Delta_L$.

$(\sigma_L^{tba} - \sigma_L^{tbe})$, not $(\{L\}^{tbe} - \{L\}^{tba})$, is the chemically significant quantity. Table 7 lists values of $(3\{L\}^{tbe} - 4\{L\}^{tba})$ which, by equation (40), is proportional to

$$(3\{L\}^{tbe} - 4\{L\}^{tba}) = \tfrac{2}{5}ce^2|Q|E_\gamma^{-1}(1 - R)\langle r^{-3}\rangle_p(\sigma_L^{tba} - \sigma_L^{tbe}) = \Delta_L \quad (40)$$

$(\sigma_L^{tba} - \sigma_L^{tbe})$. This quantity is remarkably constant; in contrast, as mentioned above $(\{L\}^{tba} - \{L\}^{tbe})$ may take either sign. Equation (41), obtained by averaging the data in Table 7, can be used to estimate either

$$(3\{L\}^{tbe} - 4\{L\}^{tba}) \approx 0.58 \text{ mm s}^{-1} \quad (41)$$

$\{L\}^{tbe}$ or $\{L\}^{tba}$ if only the other is known.

Quadrupole splittings involving less-common ligands not listed in Table 4 may often be rationalized by self-consistent arguments. Consider, for example, the $[RSn\{(OC_2H_4)_3N\}]$ and $[R_2Sn\{(OC_2H_4)_2NR'\}]$ species [28] shown in Table 8. Geometrical constraints ensure that in $[RSn\{(OC_2H_4)_3N\}]$ R and N occupy the apical positions. Thus, setting $\{R''_3N\}^{tba} = \{pip\}^{tba}$, compounds (1) to (4) in Table 8 give $\{^-C_2H_4O\}^{tbe} = -0.06$ mm s^{-1}. The

TABLE 8

^{119}Sn Mössbauer parameters of $[RSn\{(OC_2H_4)_3N\}]$ and $[R_2Sn\{(OC_2H_4)_2NR'\}]$ species *

	Compound	C.s.†/ mm s^{-1}	Q.s./ mm s^{-1}	ρ ‡
(1)	$[MeSn\{(OC_2H_4)_3N\}]$	1.04	1.64	1.58
(2)	$[EtSn\{(OC_2H_4)_3N\}]$	1.20	1.72	1.43
(3)	$[Bu^nSn\{(OC_2H_4)_3N\}]$	0.91	1.74	1.91
(4)	$[PhSn\{(OC_2H_4)_3N\}]$	0.94	1.66	1.77
(5)	$[Bu^n_2Sn\{(OC_2H_4)_2NH\}]$	0.91	2.20	2.42
(6)	$[Bu^n_2Sn\{(OC_2H_4)_2N(C_6H_4CH_3)\}]$	0.85	2.23	2.62
(7)	$[Et_2Sn\{(OC_2H_4)_2NEt\}]$	0.96	2.16	2.25

* Taken from ref. 28. † Centre shift relative to $BaSnO_3$. ‡ ρ = q.s./c.s.

quadrupole splitting then predicted for $[R_2Sn\{(OC_2H_4)_2NR'\}]$ with structure (V) is 1.95 mm s^{-1}, in agreement with observation for compounds (5) to (7).

Another interesting example is provided by the $[\{Ph_2SnO_2CR\}_2]$ dimers (Table 9), which are five-coordinate with an equatorial Sn–Sn bond and bidentate

TABLE 9

Observed and calculated quadrupole splittings in $[\{Ph_2Sn(OCOR)\}_2]$ dimers

	Compound	Obs./mm s^{-1} *	Calc./mm s^{-1}
(1)	$[Ph_4Sn_2(OAc)_2]$	3.70	†
(2)	$[Ph_4Sn_2(O{\cdot}CO{\cdot}CH_2Cl)_2]$	3.85	3.92
(3)	$[Ph_4Sn_2(O{\cdot}CO{\cdot}CCl_3)_2]$	4.10	4.16
(4)	$[Ph_4Sn_2(O{\cdot}CO{\cdot}CF_3)_2]$	4.35	4.24
(5)	$[Ph_4Sn_2(O{\cdot}COPh)_2]$	3.50	3.33 ‡

* Taken from ref. 29. † This compound used to derive $\{SnL_2R_2\}^{tbe} = -1.38$ mm s^{-1}. ‡ Calc. assuming $\{OCOPh\}^{tba} = \{bzbz\}^{tba}$.

RCO_2^- ligands bridging apical positions.[29] Thus each moiety is an R_2SnL_2M system with quadrupole splitting given by equation (42), where for the compounds in

$$|\Delta| = [7\{R\}^{tbe\,2} - 2\{R\}^{tbe}\{M\}^{tbe} + 4\{M\}^{tbe\,2} - 16\{R\}^{tbe}\{L\}^{tba} - 8\{M\}^{tbe}\{L\}^{tba} + 16\{L\}^{tba\,2}]^{\frac{1}{2}} \quad (42)$$

Table 9 R = Ph, M = SnL_2R_2, and L = AcO, $CH_2Cl{\cdot}CO_2$, $CCl_3{\cdot}CO_2$, $CF_3{\cdot}CO_2$, or $PhCO_3$. From compound (1) we

[28] A. Tzschach, K. Pönicke, L. Korecz, K. Burger, *J. Organometallic Chem.*, 1973, **59**, 199.

[29] M. Delmas, J. C. Maire, and Y. Richard, *J. Organometallic Chem.*, 1971, **30**, C101; G. Bandoli, D. A. Clemente, and C. Panattoni, *Chem. Comm.*, 1971, 311.

get $\{SnL_2R_2\}^{tbe} = -1.38$ mm s^{-1}. The splittings calculated by use of this value for compounds (2) to (5) are seen to be in good agreement with observation.

Many other illustrations could be cited. For example, in the $[R_2SnCl(S_2CNR'_2)]$ compounds [30] the observed quadrupole splittings of *ca.* 2.9 mm s^{-1} for R = alkyl are clearly consistent with the equatorial R_2SnL_3 structure (IVa), in agreement with an *X*-ray study [31] of $[Me_2SnCl(S_2CNMe_2)]$. However, although the splittings of *ca.* 2.3 mm s^{-1} for R = Ph are consistent with structure (IVa), they might also be compatible with structure (V).

Notice that throughout the data discussed in this paper there is little correlation between the quadrupole splittings and centre shifts. To illustrate this values of the ratio ρ of quadrupole splitting to centre shift relative to SnO_2 are listed in Tables 8 and 10, assuming that

TABLE 10

Values of ρ (c.s./q.s.) for some five-co-ordinate R_3SnL_2 compounds

Compound *	Q.s. †	C.s. ‡	ρ
$[Ph_3Sn(oxin)]$ [a]	1.75	1.07	1.64
$[Ph_3Sn(bzbz)]$ [b]	2.25	1.13	1.99
$[Ph_3Sn(bzac)]$ [b]	2.25	1.08	2.08
$[Ph_3Sn(ONPhCOPh)]$ [c]	1.94	1.26	1.54
$[Pr_3Sn(ONPhCOPh)]$ [c]	2.65	1.50	1.77
$[Me_3Sn(ONPhCOPh)]$ [c]	2.36	1.34	1.76
$[Me_3Sn(ONHCOPh)]$ [c]	2.74	1.37	2.00
$[Et_3NH][Ph_3Sn(ONCOPh)]$ [c]	1.74	1.23	1.41

* For abbreviations see footnotes to Tables 1 and 2. † Units are mm s^{-1}. ‡ Units are mm s^{-1}; relative to SnO_2 with $BaSnO_3$ assumed to have zero shift.

[a] Ref. 6, and R. C. Poller and J. N. R. Ruddick, *J. Chem. Soc.* (*A*), 1969, 2273. [b] Refs. 4 and 12. [c] P. G. Harrison, *Inorg. Chem.*, 1973, **12**, 1545.

$BaSnO_3$ has zero shift relative to SnO_2. The ratio ρ has been suggested [32] as an index of co-ordination number, with ρ > *ca.* 2.1 characteristic of co-ordination numbers greater than four. However, the data show that ρ varies above and below 2.1 even in closely related compounds.

Partial Quadrupole Splitting Parameters for $^{121}Sb^{V}$.—Quadrupole coupling in the ground state ($I = \frac{5}{2}$, $Q < 0$) of ^{121}Sb may be observed by Mössbauer or n.m.r./n.q.r. spectroscopy. Partial quadrupole splitting parameters for $^{121}Sb^{V}$, corresponding to Scheme (*A*) (see earlier), are defined (in units of mm s^{-1} for the 37.15 keV $\frac{5}{2}^+ \leftrightarrow \frac{7}{2}^+$ Mössbauer resonance) by equations (43) and (44). The factor of $\frac{1}{2}$ is omitted for ^{121}Sb since experimental data are presented as the 'coupling constant' e^2qQ, whereas with ^{119}Sn only the 'quadrupole splitting' $\frac{1}{2}e^2qQ(1 + \frac{1}{3}\eta^2)^{\frac{1}{2}}$ is measured in routine experiments.

$$\{L\}^{tba} = ce^2|Q|E_\gamma^{-1}([L]^{tba} - [X]^{tba}) \quad (43)$$

$$\{L\}^{tbe} = ce^2|Q|E_\gamma^{-1}([L]^{tbe} - \tfrac{4}{3}[X]^{tba}) \quad (44)$$

Studies of isoelectronic isostructural $^{119}Sn^{IV}$ and $^{121}Sb^{V}$ compounds show that ^{121}Sb coupling constants are +6.76 times the corresponding ^{119}Sn quadrupole splittings.[5,6] In Table 11 p.q.s. parameters obtained by multiplying the ^{119}Sn values by 6.76 are compared with the values obtained by *ad hoc* methods.[7] Except for $\{Ph\}^{tba}$ (which is discussed later) the two procedures are mostly in good agreement, with our results resolving the previous ambiguity concerning the sign of $\{Cl\}^{tbe}$.

TABLE 11

Estimated p.q.s. parameters for trigonal-bipyramidal organoantimony(V) compounds *

	$\{L\}^{tba}$/mm s^{-1}		$\{L\}^{tbe}$/mm s^{-1}	
Ligand	This work †	Ref. 7	This work †	Ref. 7
Cl	0 ‡	0 ‡	+1.34 ‡	±0.9
Br	0 ‡	−0.2	+1.34 ‡	
Alkyl	−6.37		−7.62	−8.0
Ph	−6.00	−7.2	−6.62	−6.9
F	+0.75	+0.3		
I	−0.54	−0.7		
NO_3	+0.75	+0.2		
NCS	+0.44	−0.1		
OAc	+0.51			
OH	−0.87	−0.3		

* $\{L\}^{tba}$ and $\{L\}^{tbe}$ for ^{121}Sb are defined in equations (43) and (44). For the ^{121}Sb 37.15 keV Mössbauer resonance 1 mm s^{-1} = 29.96 MHz. † 6.76 × [^{119}Sn p.q.s. parameter given in Table 4]. ‡ Here and in ref. 7 $\{Cl\}^{tba} = 0$ by definition; we also take $\{Br\} \equiv \{Cl\}$ for both tba and tbe.

The larger scale of ^{121}Sb quadrupole couplings means that tolerance limits for the additive model must be greater than the ±0.4 mm s^{-1} used for ^{119}Sn. However, there is no obvious theoretical reason why they should be greater by exactly the same factor as the coupling constants (*i.e.* ±0.4 × 6.76 = ±2.7 mm s^{-1}), since neither systematic errors (*e.g.* distortions) nor experimental errors are necessarily proportional to the quadrupole interaction.

In Table 12 coupling constants calculated by use of ^{119}Sn-derived p.q.s. parameters are compared with observed values [7,33] for a number of trigonal-bipyramidal Sb^{V} compounds. The agreement for R_3SbL_2 species is excellent, with no evidence of bias in the calculated values. However, in the Ph_4SbL species although agreement is always to within 3 mm s^{-1}, our calculated values consistently overestimate (in magnitude) the observed coupling constants. The statistic *t* [equations (38) and (39)] takes the value −5.5 on 5 degrees of freedom, which is clearly significant since $|t| \geqslant 5.5$ has a probability less than 0.05% of occurring by chance. Inspection of Table 11 reveals that this discrepancy arises because our value of 6.00 mm s^{-1} for $|\{Ph\}^{tba}|$ is distinctly smaller than the value of 7.2 mm s^{-1} obtained in ref. 7 from the coupling constant observed in $[Ph_4SbCl]$. To obtain the proportionality between ^{119}Sn and ^{121}Sb the larger value would require $\{Ph\}^{tba} = -1.06$ mm s^{-1} for ^{119}Sn. However, the ^{119}Sn data discussed provide no support for the hypothesis that $|\{Ph\}^{tba}|$ should be increased by this amount. (Our

[30] B. W. Fitzsimmons and A. C. Sawbridge, *J.C.S. Dalton*, 1972, 1678.

[31] K. Furue, T. Kimura, N. Yasuoka, N. Kasai, and M. Kakudo, *Bull. Chem. Soc. Japan*, 1970, **43**, 1661.

[32] R. H. Herber, H. A. Stockler, and W. T. Reichle, *J. Chem. Phys.*, 1965, **42**, 2447.

[33] G. G. Long, J. G. Stevens, R. J. Tullbane, and L. H. Bowen, *J. Amer. Chem. Soc.*, 1970, **92**, 4230.

remarks above concerning bias in Table 6 seem mere quibbles in the present context, and anyway have implications for $\{Ph\}^{tbe}$ rather than $\{Ph\}^{tba}$.) Thus it seems that apical Sn–Ph and Sb–Ph bonds are not strictly comparable.

TABLE 12

Observed and calculated quadrupole coupling constants (ce^2qQ/E_γ in mm s^{-1}) for some organoantimony(V) compounds

	Compound	Obs.[a]	Calc.[b] This work	Calc.[b] Ref. 7
(1)	$[Ph_3SbF_2]$	−22.0	−22.8	*c*
(2)	$[Ph_3SbCl_2]$	−20.6	−19.9	*c*
(3)	$[Ph_3SbBr_2]$	−19.8	−19.9	*c*
(4)	$[Ph_3SbI_2]$	−18.1	−17.7	*c*
(5)	$]Ph_3Sb(NO_3)_2]$	−21.3	−22.8	*c*
(6)	$[Ph_3Sb(NCS)_2]$	−20.4	−21.6	*c*
(7)	$[Ph_3Sb(OAc)_2]$	−20.9[d]	−21.9	
(8)	$[Me_3SbCl_2]$	−24.0	−22.9	*c*
(9)	$[Me_3SbBr_2]$	−22.1	−22.9	−23.2
(10)	$[Ph_4SbF]$	−7.2	−9.4	−6.9
(11)	$[Ph_4SbCl]$	−6.2	−7.9	*c*
(12)	$[Ph_4SbBr]$	−6.8	−7.9	−5.9
(13)	$[Ph_4SbNO_3]$	−6.4	−9.4	−6.7
(14)	$[Ph_4SbOH]$	−5.3	−6.1	*c*
(15)	$[Ph_4SbNCS]$	−6.4	−8.7	−6.1[e]

[a] Refs. 7 and 33; absorbers at 4.2 (ref. 33) or 9 K (ref. 7); $\eta = 0.0$ unless otherwise noted. [b] Assuming ideal trigonal-bipyramidal geometry with electronegative ligands apical. [c] In ref. 7 these coupling constants were used to calculate p.q.s. parameters. [d] $\eta = 0.29$; an alternative fit with $\eta = 0$, $|ce^2qQE_\gamma^{-1}| = 21.8$ mm s^{-1} was equally acceptable. [e] This number appears to be misprinted in ref. 7.

The alternative hypothesis that in Sb^V compounds the p.q.s. of an electronegative ligand L is affected by a *trans* phenyl group is less likely. First, the discrepancy between the two methods of calculation is much greater for $\{Ph\}^{tba}$ than for any of the other p.q.s. parameters listed in Table 11, including $\{OH\}^{tba}$ which in ref. 7 was deduced from the coupling constant observed in $[Ph_4SbOH]$. Secondly the structural data given in Table 13 show that Sb–O bond lengths are scarcely changed by a *trans* phenyl.

TABLE 13

Metal–ligand bond lengths in some trigonal-bipyramidal Sn^{IV} and Sb^V compounds

Compound *	M–C/Å Equatorial †	M–C/Å Apical	M–O/Å Apical †
$[Ph_4SbOH]$[a]	2.128	2.218	2.048
$[Ph_4SbOMe]$[b]	2.118	2.199	2.061
$[Ph_3Sb(OMe)_2]$[b]	2.120		2.033
$[Ph_5Sb]\cdot\frac{1}{2}C_6H_{12}$[c]	2.14	2.24	
$[Ph_3Sn(bzbz)]$[c]	2.165	2.180	2.276
$[Ph_3Sn(ONPhCOPh)]$[d]	2.14	2.18	2.31

* For abbreviations see footnotes to Tables 1 and 2. † Averaged where appropriate.

[a] A. L. Beauchamp, M. J. Bennett, and F. A. Cotton, *J. Amer. Chem. Soc.*, 1969, **91**, 297. [b] K-W. Shen, W. E. McEwen, S. J. LaPlaca, W. C. Hamilton, and A. P. Wolf, *J. Amer. Chem. Soc.*, 1968, **90**, 1718. [c] Ref. 12. [d] T. J. King and P. G. Harrison, *J.C.S. Chem. Comm.*, 1972, 815. [e] C. Brabant, B. Blanck, and A. Beauchamp, *J. Organometallic Chem.*, 1974, **82**, 231.

Inspection of Table 13 also reveals that the difference between apical and equatorial Sb–C distances at *ca.* 0.09 Å is somewhat larger than the difference of *ca.* 0.03 Å observed for the two Sn^{IV} compounds listed. The (perhaps unexpected) possibility that, for a given ligand A, larger σ_A values seem to be associated with longer bonds also follows from the positive ($\sigma_A^{tba} - \sigma_A^{tbe}$) values noted in Table 7, since apical tin–ligand bonds tend to be longer than equatorial ones.[13] However, it is very difficult to assess the validity of this point because the relationship of bond length to partial field gradients is inextricably mixed with other factors.

Finally, the ambiguity (discussed in ref. 7) between five- and six-co-ordinate structures for $[Ph_2SbCl_3]$ may be resolved by the methods used in this section. From Table 11 the calculated coupling constant for a trigonal-bipyramidal structure with equatorial phenyl groups is +17.9 mm s^{-1}, whereas the coupling constant for a *trans*-phenyl octahedral structure with bridging chlorines is calculated from the corresponding ^{119}Sn case[1] as $+4 \times 0.95 \times 6.76 = +25.7$ mm s^{-1}. The observed value[7] of +25.9 mm s^{-1} is in good agreement with the octahedral structure; in contrast, the trigonal-bipyramidal structure would be rejected at any realistic tolerance limit.

Conclusion.—This paper essentially completes the additive treatment of $^{119}Sn^{IV}$ Mössbauer quadrupole splittings in terms of the MO model developed in ref. 1. The different p.q.s. parameters for tetrahedral, trigonal-bipyramidal, and octahedral structures seem to give a very consistent description of the relationship between quadrupole splitting and stereochemistry in organotin(IV) compounds, in spite of distortions from ideal geometry. From Figure 2 it is seen that quadrupole splittings in $[R_3SnL_2]$ span almost the entire range of splittings observed in tetrahedral $[R_3SnL]$ and octahedral $[R_2SnL_4]$ species. This emphasizes that in general a particular range of quadrupole splittings cannot be uniquely associated with a particular stereochemistry, and that reliable structural information can only be deduced by use of either unbiassed p.q.s. values or a regression method of the type outlined. Further, statistical methods properly combined with chemical judgement can provide a quantitative guide to the probable correctness of predictions based on the additive model. In particular, our strategy of averaging over distortions from ideal geometry means that these effects, which are not included in the additive model, are reflected in pseudo-random 'errors' which can be used to construct tolerance limits.

APPENDIX (1)

To illustrate the tactics used in deriving equations (15), (16), and other results given in this paper, we present the detailed working for equation (15). The symmetrized parameter[18] S_{02} is especially useful in this and other derivations in this paper.

If equations (8)—(10) are multiplied by $\frac{1}{2}ce^2|Q|E_\gamma^{-1}$ and the right-hand sides expressed in terms of p.q.s.

parameters, we get equations (A1)—(A3), where $\Delta_{xx}^{\mathrm{II}} = \frac{1}{2}ce|Q|E_\gamma^{-1}V_{xx}^{\mathrm{II}}$, *etc.* Also, remembering that $Q < 0$,

$$\Delta_{xx}^{\mathrm{II}} = -\{\mathrm{R}\}^{\mathrm{tba}} - \tfrac{1}{2}\{\mathrm{R}\}^{\mathrm{tbe}} - \{\mathrm{L}\}^{\mathrm{tba}} + 2\{\mathrm{L}\}^{\mathrm{tbe}} \quad (\mathrm{A1})$$

$$\Delta_{yy}^{\mathrm{II}} = -\{\mathrm{R}\}^{\mathrm{tba}} + \tfrac{5}{2}\{\mathrm{R}\}^{\mathrm{tbe}} - \{\mathrm{L}\}^{\mathrm{tba}} - \{\mathrm{L}\}^{\mathrm{tbe}} \quad (\mathrm{A2})$$

$$\Delta_{zz}^{\mathrm{II}} = 2\{\mathrm{R}\}^{\mathrm{tba}} - 2\{\mathrm{R}\}^{\mathrm{tbe}} + 2\{\mathrm{L}\}^{\mathrm{tba}} - \{\mathrm{L}\}^{\mathrm{tbe}} \quad (\mathrm{A3})$$

$m(\mathrm{R,L})\Delta_0$, Δ_{R}, and Δ_{L} [see equations (4), (5), and (14)] can be expressed in terms of p.q.s. parameters by equations (A4)—(A6).

$$m(\mathrm{R,L})\Delta_0 = 4\{\mathrm{L}\}^{\mathrm{tba}} - 4\{\mathrm{R}\}^{\mathrm{tba}} \quad (\mathrm{A4})$$

$$\Delta_{\mathrm{R}} = 4\{\mathrm{R}\}^{\mathrm{tbe}} - 4\{\mathrm{R}\}^{\mathrm{tba}} \quad (\mathrm{A5})$$

$$\Delta_{\mathrm{L}} = 3\{\mathrm{L}\}^{\mathrm{tbe}} - 4\{\mathrm{L}\}^{\mathrm{tba}} \quad (\mathrm{A6})$$

Next, three of the four p.q.s. parameters in equations (A4)—(A6) are expressed in terms of the fourth. For example, taking $\{\mathrm{L}\}^{\mathrm{tba}}$ as the fourth we get equations (A7)—(A9). When these equations are substituted into

$$\{\mathrm{R}\}^{\mathrm{tba}} = -\tfrac{1}{4}m\Delta_0 + \{\mathrm{L}\}^{\mathrm{tba}} \quad (\mathrm{A7})$$

$$\{\mathrm{R}\}^{\mathrm{tbe}} = \tfrac{1}{3}(\Delta_{\mathrm{R}} - m\Delta_0) + \tfrac{4}{3}\{\mathrm{L}\}^{\mathrm{tba}} \quad (\mathrm{A8})$$

$$\{\mathrm{L}\}^{\mathrm{tbe}} = \tfrac{1}{3}\Delta_{\mathrm{L}} + \tfrac{4}{3}\{\mathrm{L}\}^{\mathrm{tba}} \quad (\mathrm{A9})$$

equations (A1)—(A3) the terms in $\{\mathrm{L}\}^{\mathrm{tba}}$ cancel out, and we get equations (A10)—(A12).

$$\Delta_{xx}^{\mathrm{II}} = +\tfrac{5}{12}m\Delta_0 - \tfrac{1}{6}\Delta_{\mathrm{R}} + \tfrac{2}{3}\Delta_{\mathrm{L}} \quad (\mathrm{A10})$$

$$\Delta_{yy}^{\mathrm{II}} = -\tfrac{7}{12}m\Delta_0 + \tfrac{5}{6}\Delta_{\mathrm{R}} - \tfrac{1}{3}\Delta_{\mathrm{L}} \quad (\mathrm{A11})$$

$$\Delta_{zz}^{\mathrm{II}} = +\tfrac{1}{6}m\Delta_0 - \tfrac{2}{3}\Delta_{\mathrm{R}} - \tfrac{1}{3}\Delta_{\mathrm{L}} \quad (\mathrm{A12})$$

The expression [18] for $|\Delta_{\mathrm{II}}|$ in terms of S_{02} gives equation (A13), and on substituting from equations (A10)—(A12)

$$|\Delta_{\mathrm{II}}| = (-\tfrac{4}{3}S_{02})^{\frac{1}{2}} = [-\tfrac{4}{3}(\Delta_{xx}^{\mathrm{II}}\Delta_{yy}^{\mathrm{II}} + \Delta_{yy}^{\mathrm{II}}\Delta_{zz}^{\mathrm{II}} + \Delta_{xx}^{\mathrm{II}}\Delta_{zz}^{\mathrm{II}})]^{\frac{1}{2}} = [\tfrac{4}{3}(\Delta_{zz}^{\mathrm{II}\,2} - \Delta_{xx}^{\mathrm{II}}\Delta_{yy}^{\mathrm{II}})]^{\frac{1}{2}} \quad (\mathrm{A13})$$

the exact result equation (15*a*) is obtained. This is linearized by use of the binomial theorem to give (15*b*),

$$|\Delta_{\mathrm{II}}| = \tfrac{1}{3}[\tfrac{13}{4}(m\Delta_0)^2 - 8(m\Delta_0)\Delta_{\mathrm{R}} + 5(m\Delta_0)\Delta_{\mathrm{L}} + 7\Delta_{\mathrm{R}}^2 - 2\Delta_{\mathrm{R}}\Delta_{\mathrm{L}} + 4\Delta_{\mathrm{L}}^2]^{\frac{1}{2}} \quad (15a)$$

$$= \frac{\sqrt{13}}{6}|m\Delta_0|[1 - \frac{32\Delta_{\mathrm{R}}}{13m\Delta_0} + \frac{20\Delta_{\mathrm{L}}}{13m\Delta_0} + \text{smaller terms}]^{\frac{1}{2}}$$

$$= \frac{\sqrt{13}}{6}m|\Delta_0| - \frac{8}{3\sqrt{13}}\Delta_{\mathrm{R}} + \frac{5}{3\sqrt{13}}\Delta_{\mathrm{L}} \quad (15b)$$

remembering that $m(\mathrm{R,L})$ and Δ_0 are both positive.

The derivations of equations (16), (27), (28), (31)—(34), (36), (37), and (42) all involve similar methods.

APPENDIX (2)

The following proof, suggested by A. J. Stone of the University of Cambridge, is given here as an illustration of how the likelihood function [34] provides a powerful yet simple method for constructing the proofs of statistical results required in work of the type described in this paper.

For a set of N data points (x_i, y_i) consider the alternative hypotheses that either ($H1$) the points belong to a given regression line about which they are normally-distributed at perpendicular distances p_i with standard deviation σ, or ($H2$) the points belong to another line displaced a distance μ from the given line, and are normally distributed about the displaced line at distances $(p_i - \mu)$ with standard deviation σ. The likelihood functions for these two hypotheses are shown in equations (A14) and (A15), where C is

$$L_1 = C\sigma^{-N}\exp(-\sum_i p_i^2/2\sigma^2) \quad (\mathrm{A14})$$

$$L_2 = C\sigma^{-N}\exp(-\sum_i (p_i - \mu)^2/2\sigma^2) \quad (\mathrm{A15})$$

an unknown constant. The difference in support ($S = \ln L$) for the two hypotheses is given by equation (A16). Support

$$S_2 - S_1 = \sum_i [p_i^2 - (p_i - \mu)^2]/2\sigma^2 \quad (\mathrm{A16})$$

for ($H2$) relative to ($H1$) is maximized if $(S_2 - S_1)$ is maximized, *i.e.* if $\mu = \bar{p} = \Sigma_i p_i/N$. In this case we have equation (A17).

$$(S_2 - S_1)^{\max} = N\bar{p}^2/2\sigma^2 \quad (\mathrm{A17})$$

Suppose ($H2$) is adopted in preference to ($H1$) only if $(S_2 - S_1)^{\max} \geqslant w$ units of support. Then ($H2$) will be adopted if $N\bar{p}^2/2\sigma^2 \geqslant w$, *i.e.* if equation (A18) holds.

$$|\bar{p}| \geqslant (2w)^{\frac{1}{2}}\sigma/N^{\frac{1}{2}} \quad (\mathrm{A18})$$

This proves the result cited in the text, namely that tolerance limits for the mean of the perpendicular displacements of N observations are $N^{-\frac{1}{2}}$ times those for one observation.

In the general case, for a given line making an angle θ_1 with the x axis ($H2$) is replaced by the hypothesis that the points belong to a line obtained from the given line by rotation through an angle $(\theta_2 - \theta_1)$ and displacement by a distance μ. The origin for the rotation is the centre of gravity of the data used to construct the original line, *i.e.* the point such that the original line has the equation $Y = X\tan\theta_1$. The maximum support available for ($H2$) over ($H1$) is then given by equation (A19), where $\langle \ldots \rangle$

$$(S_2 - S_1)^{\max} = (N/2\sigma^2)[\bar{p}^2 + \{\langle(x - \bar{x})^2\rangle - \langle(y - \bar{y})^2\rangle\}\sin(\theta_1 + \theta_2)\sin(\theta_1 - \theta_2) - 2\langle(x - \bar{x})(y - \bar{y})\rangle\cos(\theta_1 + \theta_2)\sin(\theta_1 - \theta_2)] \quad (\mathrm{A19})$$

and $\overline{\cdots}$ both denote the arithmetic mean, and θ_2 is a root of equation (A20). It is seen that the support available

$$(\tan^2\theta_2 - 1)\langle(x - \bar{x})(y - \bar{y})\rangle + [\langle(x - \bar{x})^2\rangle - \langle(y - \bar{y})^2\rangle]\tan\theta_2 = 0 \quad (\mathrm{A20})$$

now depends both on the displacement of the centre of gravity of the new points, and on their dispersion about this centre of gravity. In general, tolerance limits obtained from equation (A19) will vary with position along the original line. However, for the applications described in this paper $|\theta_2 - \theta_1|$ is not large and it is preferable to use only perpendicular-displacement tolerance limits based on equation (A17). Any resulting error [which tends to favour retaining ($H1$)] is more than outweighed by convenience of application. Note that in any case for a single new point, $N = 1$, equation (A19) for $(S_2 - S_1)^{\max}$ reduces to equation (A17).

We thank the N.R.C. (Canada) for financial support. The work described in this paper was initiated while one author (M. G. C.) was at the University Chemical Laboratory, Cambridge.

[5/515 *Received*, 17*th March*, 1975]

[34] Ref. 21, sect. 10.10; ref. 22, especially chs. 2 and 3.